

Data-Assisted Model-Based Anomaly Detection for High-Fidelity Simulators of Power Systems

KAIKAI PAN, PETER PALENSKY, AND PEYMAN MOHAJERIN ESFAHANI

ABSTRACT. The main objective of this article is to develop scalable anomaly detectors for high-fidelity simulators of power systems. On the one hand, high-fidelity models are typically too complex to apply existing model-based approaches in the fault/anomaly detection literature. On the other hand, pure data-driven approaches developed primarily in the machine learning literature neglect our knowledge about the underlying dynamics of power systems. To address these shortcomings, we develop a data-assisted model-based diagnosis filter that utilizes both the model-based knowledge and also the simulation data from the simulator. The diagnosis filter aims to achieve two desired features: (i) performance robustness with respect to output mismatches; (ii) high scalability. To this end, we propose a tractable optimization-based reformulation in which decisions are the filter parameters, the model-based information introduces feasible sets, and the data from the simulator forms the objective function to-be-minimized regarding the effects of output mismatches on the filter performance. To validate the theoretical results and its effectiveness, we implement the developed diagnosis filter in DIGSILENT PowerFactory to detect false data injection attacks on the Automatic Generation Control measurements in the three-area IEEE 39-bus system.

1. INTRODUCTION

The principle of anomaly detection in power system cyber security is to generate a diagnostic signal (e.g., residual) which keeps sensitive to attacks but decoupled from other unknowns, given the available data from system outputs. The detection methods can be mainly classified into two categories: (i) the approaches that exploit the explicit mathematical model of the system dynamics (referred to *model-based* methods in this article); (ii) the *data-driven* approaches that try to automatically learn the system characteristics from the output data [17, 24]. Our work in [18] has developed a diagnosis tool to detect the class of multivariate false data injection (FDI) attacks that may remain stealthy in view of a static detector, by capturing the dynamics signatures of such a disruptive intrusion. This method is, indeed, model-based that the dynamics of the system trajectories under the multivariate attacks are described via an explicit mathematical model representation (i.e., linear differential-algebraic equations (DAEs)). The numerical results in [18] have proven its effectiveness in the linearized mathematical model. Now here comes another question:

Can the power of scalable model-based diagnosis tools be still utilized in real-world applications such as electric power systems for which there are reliable datasets from high-fidelity but complex simulators?

Literature on model-based and data-driven anomaly detection. Our objective in this article is to address this question. Before answering that, we first provide a brief overview on the model-based and data-driven detectors. In fact, both types have their own advantages and limitations. The model-based methods require that the system dynamics must be well understood [21]. Observer-based residual generator is a major subclass of these schemes. The modeling framework has been extended to general linear DAEs as many

Date: April 30, 2020.

The authors are with the Delft University of Technology, The Netherlands (email: {K.Pan, P.Palensky, P.MohajerinEsfahani}@tudelft.nl).

governing physical laws of power systems are made through differential equations [15, 2]. Parity space [16] and parameter estimation [8] model-based methods have also been extensively investigated. For instance, the extended Kalman filter algorithm is used to perform such an estimation for anomaly detection [9]. The residual generators above usually have the same degree as the system dynamics, which can be problematic in the online implementation particularly for large-scale power systems [5]. Our diagnosis filter in [18] provides a good alternative to detect the disruptive multivariate attacks in a real-time operation. Still, the challenge remains as the power system models are mostly nonlinear, complex and high-dimensional. The work in [12] proposed an optimization-based filter for detecting a single fault in the scenario where the nonlinearity in the control system model can be fully described. However, developing accurate mathematical models with all the details of nonlinearities and uncertainties in power systems is usually difficult (or even infeasible), especially in the case that some uncertainties can not be well quantified [22].

Another major technique for anomaly detection comes from data-driven approaches which do not require an explicit mathematical model of the system dynamics. Developments such as sensing technology, Internet-of-Things and Artificial Intelligence have contributed to a more data-driven power system. Anomaly detection is mainly considered as a classification problem and there are supervised or unsupervised learning approaches for that purpose. Among all the supervised classifications, deep neural networks (DNN) [25, 3], bayesian networks [23] and Kernel machines [17] are the popular methods. For unsupervised classifications, one can find principle component analysis (PCA) and its extensions [10, 6], autoencoders [1], etc. In addition to supervised or unsupervised approaches, recent work in [11] has proposed a reinforcement learning based algorithm for online attack detection without a prior knowledge of the system models or attack types. Overall, data-driven methods are suitable for complex and large-scale power systems. However, their performance highly depends on the quantity and quality of the accessible data [22], and thus can be intractable in many cases. Besides, the required pre-processing stage (e.g., data training) may have a high computational cost.

Contributions and outline. This article aims to develop a scalable diagnosis filter for a high-fidelity but complex simulator (e.g., DIgSILENT PowerFactory (PF)). We still utilize the model-based information to build up a scalable filter design. But as noted earlier, *output mismatches* can be observed from the output of the mathematical model in model-based detection and the one from the high-fidelity simulator. In this regard, we propose a tractable optimization-based reformulation where the model-based information introduces feasible sets, and the simulation data forms the objective function to minimize the effects of output mismatches on the filter performance. In this way, the diagnosis filter can be “trained” in the normal operations (without attacks) to have performance robustness with respect to the output mismatches. Then the robustified diagnosis filter can be “tested” in PF to detect the occurrence of FDI attacks. Our main contributions are:

- (i) Firstly, we depart from the pure model-based or data-driven viewpoints to develop a diagnosis filter which uses both the model-based knowledge for a scalable design and the simulation data to robustify itself to the output mismatches, yielding a novel data-assisted model-based approach. To quantify the effects of output mismatches, a square of \mathcal{L}_2 -inner product with corresponding norm is introduced for the discrete-time signal in a finite time horizon. Subsequently, a robustification scheme in the “training” phase is formulated as an optimization program where the effects of output mismatches on the filter performance are minimized and the filter scalability are achieved (Definition 3.1 and Remark 3.2).
- (ii) We investigate the tractable optimization-based characterization of the diagnosis filter in both scenarios of univariate and multivariate attacks. The \mathcal{L}_2 -norm of the residual part introduced by output mismatches is reformulated as a quadratic function, and we further propose quadratic programming characterization for the robust diagnosis filter under the univariate attack. The resulted filter can

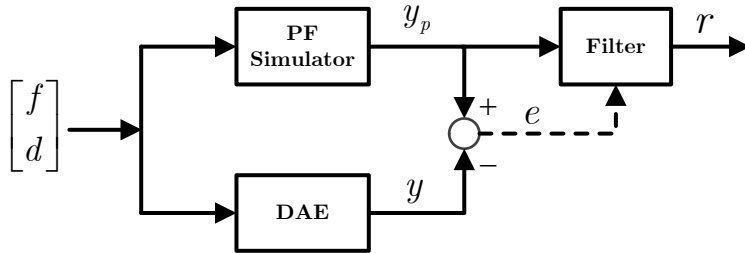


FIGURE 1. Configuration of the proposed solution.

even have non-zero steady-state residual that tracks the univariate attack value (Theorem 3.3). We also extend the robust diagnosis filter design to solve the detection problem of multivariate attacks. (Corollary 3.4).

The process of diagnosis filter construction and validation is concluded in Algorithm 1. Besides, the effectiveness of the proposed approach is validated on the three-area IEEE 39-bus system. Numerical results from the case study illustrate that the robust diagnosis filter for the PF simulator can successfully generate alerts in the presence of FDI attacks, while a filter without such a robustification scheme may fail.

Section 2 presents the outline of our proposed solution. Both mathematical framework and motivating case study are detailed described. Section 3 proposes the tractable optimization-based characterization of the diagnosis filter which has high scalability and performance robustness to the output mismatches. Numerical results of the robust diagnosis filter in the case study are reported in Section 4.

2. OUTLINE OF THE PROPOSED SOLUTION

In this section, the mathematical framework of our proposed solution to design a diagnosis filter for the high-fidelity simulator will be presented. We will also provide the motivating case study in power systems to illustrate such a process.

2.1. Mathematical framework

The configuration of our approach to develop a diagnosis filter for the high-fidelity simulator (i.e., PF) is presented in Figure 1. We aim to develop a filter which can generate a diagnostic signal (i.e., residual r) to differentiate whether the measurements are a consequence of the normal disturbance input d , or due to the anomaly signal f , given the available output data y_p from the PF simulator. Besides, our proposed solution builds on a new data-assisted model-based perspective that the filter utilizes not only the model-based information for a scalable design but also the simulation data to “train” the filter to achieve performance robustness to the output mismatches which can be characterized by e . Now we provide the mathematical framework for the corresponding elements in Figure 1 of the filter configuration.

Let us start with the description of the mathematical model which is commonly used in the model-based detection. This model-based information will provide feasible sets for the diagnosis filter design of this article. Let us consider the following DAE model in the setup of Figure 1,

$$H(q)x[k] + L(q)y[k] + F(q)f[k] = 0, \quad (1)$$

where $x[k] \in \mathbb{R}^{n_x}$ represents the unknown signals such as the internal system states and natural disturbances, $y[k] \in \mathbb{R}^{n_y}$ contains all the system outputs for the anomaly detection purpose, and $f[k] \in \mathbb{R}^{n_f}$ stands for the anomalies (e.g., FDI attacks) which are the targets of detection. The operator q can be treated as a type

of time-shift operator that $qx[k] \rightarrow x[k+1]$ for the time step $k \in \mathbb{N}$, and H, L, F are polynomial matrices in terms of the operator q with n_r rows and n_x, n_y, n_f columns separately. In what follows we show the generality of the DAE model in (1) by introducing the example of a classical linear state-space representation of the system dynamics,

$$\begin{cases} X[k+1] = AX[k] + B_d d[k] + B_f f[k], \\ Y[k] = CX[k] + D_f f[k], \end{cases} \quad (2)$$

where $X[k] \in \mathbb{R}^{n_x}$ is the system state, $Y[k] \in \mathbb{R}^{n_y}$ is the measured output. The system input signals contain the natural disturbances $d[k] \in \mathbb{R}^{n_d}$ and the anomalies $f[k]$. Besides, A, B_d, B_u, C and D_f are constant matrices with appropriate dimensions. In light of (1) and (2), we can let $x := [X^\top d^\top]^\top$ for the unknown signals and $y := Y$ for the system outputs such that (2) can be easily fitted into (1), by defining,

$$H(q) := \begin{bmatrix} -qI + A & B_d \\ C & 0 \end{bmatrix}, \quad L(q) := \begin{bmatrix} 0 \\ -I \end{bmatrix}, \quad F(q) := \begin{bmatrix} B_f \\ D_f \end{bmatrix}.$$

Note that the framework above is rich enough to subsume the system dynamics models of interest. In fact, let us consider a typical closed-loop system where the electric power system is operated by a dynamic controller that receives the measurements as inputs and sends control signals to the actuators through communication networks which may be exposed to cyber attacks. Then when an FDI attack corrupts the measurements, it affects the dynamics of the controller and consequently the involved power system. To study its behavior, we can augment the physical system dynamics with the controller states and outputs, and a linear mathematical model with augmented states and outputs can be derived in the form of (2) which again can be fitted into the DAE model (1). In the next subsection we will provide such an example in the motivating case study. Moreover, throughout this article we focus on the discrete-time models, but one can obtain similar results for continuous-time models by changing the operator q in (1) to the distributional derivative operator [12].

Next, for the filter design in Figure 1, the outputs y_p from the simulation results of the PF simulator are available as inputs for the diagnosis task. In this article, we propose a linear time invariant diagnosis filter as a type of residual generator which has a linear transfer operator, i.e.,

$$r[k] := R(q)y_p[k], \quad (3)$$

where the parameter $R(q)$ with a predefined order is the design variable of the diagnosis filter. Unlike many observer-based methods, the order of $R(q)$ here can be much less than the dynamical system degrees, which is always more desired for the online implementations in practice; see Section 4.

To highlight, our data-assisted model-based approach utilizes the model-based information from the DAE framework in the preceding to introduce feasible sets for the design variable $R(q)$. Due to the mismatch of the DAE model and the one in the high-fidelity simulator, output mismatches can be observed from the simulation results, and we use the simulation data to extract such output mismatch signatures as follows,

$$e[k] = y_p[k] - y[k], \quad \forall k \in \mathbb{N}. \quad (4)$$

Note that y is the output of the DAE model in (1). As shown in Figure 1, our proposed solution which further has a tractable optimization-based characterization would use such signatures information from the simulation data to form an objective function to-be-minimized regarding the effects of output mismatches on the filter residual r . We will present the details of our proposed solution in Section 3.

2.2. Motivating case study: AGC modeled in PowerFactory

A motivating case study within the power systems can be the Automatic Generation Control (AGC) model under cyber attacks. We will provide its DAE description and also the modeling process in the high-fidelity PF

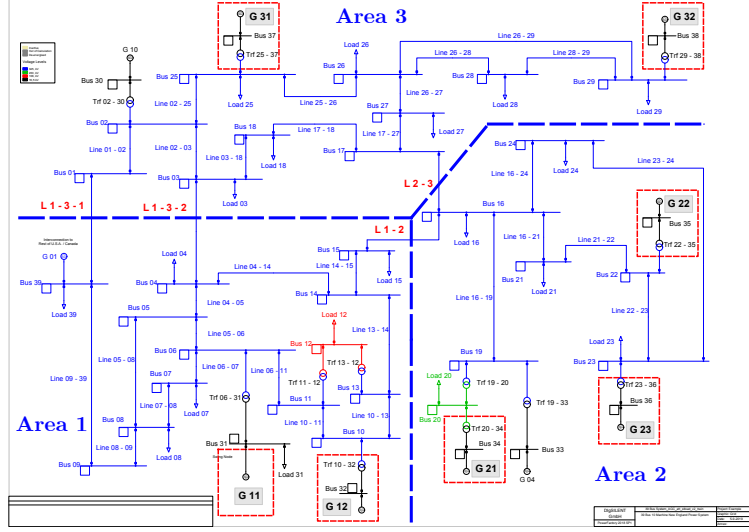


FIGURE 2. Three-area system with AGC functions in the PF.

simulator. The AGC is an automatic closed-loop system that regulates the power grid frequency. For a multi-area power system, the AGC block in each area collects the frequency and tie-line power flow measurements and sends control signals to the participating generators. After receiving the measurements, Area i would calculate an area control error (ACE) signal,

$$ACE_i = \beta_i(\omega_i - \omega_0) + (P_{tie_i} - P_{tie_0}), \quad (5)$$

where β_i is the frequency bias, ω_i and P_{tie_i} denote the frequency and tie-line power flow measurements of Area i , and ω_0 and P_{tie_0} correspond to the nominal or scheduled values. The ACE value defines the frequency to restore and the power to compensate in the event of load-generation imbalance. With the input of ACE_i , the AGC controller generates a control signal for Area i . This is usually a integral action, i.e.,

$$\Delta \dot{P}_{agc_i} = K_{I_i} ACE_i, \quad (6)$$

where K_{I_i} is the integral coefficient and ΔP_{agc_i} is the control signal that is feeding into the governors of the generators in Area i according to each generator's participating factor.

The measurements and control signals above are usually transmitted through the typical supervisory control and data acquisition (SCADA) communication networks, which are still largely based on legacy technology, and thus are vulnerable to cyber intrusions [19, 7]. For instance, an FDI attack can manipulate some tie-line power flow measurements to corrupt the AGC process and consequently the system frequency stability. In the work of such an analysis, each area of a power system is usually represented by a linearized model comprised of equivalent rotating mass, governors and turbines [2]. With the linearized model and the linear equations for corrupted AGC signals, the mathematical description of the AGC system under FDI attacks can be derived in the form of (2) after *discretization*. We omit the details as this model information can be found in a lot of existing work [2, 14].

Next, we also build the high-fidelity simulation model in the simulator PF for the 39-bus system equipped with AGC functions. As shown in Figure 2, the 39-bus transmission network is divided into three areas: Area 1 consists of 2 generators (G 11, G 12) participating in AGC and 7 loads; Area 2 has 3 generators (G 21, G 22, G 23) for AGC operations and 5 loads; Area 3 contains 2 generators (G 31, G 32) for AGC and 7 loads. Transmission lines called tie-lines (L 1-3-1, L 1-3-2, L 1-2, L 2-3) connect areas. In the simulations, the dynamic generator model consists of a synchronous machine, along with automatic voltage regulator (AVR)

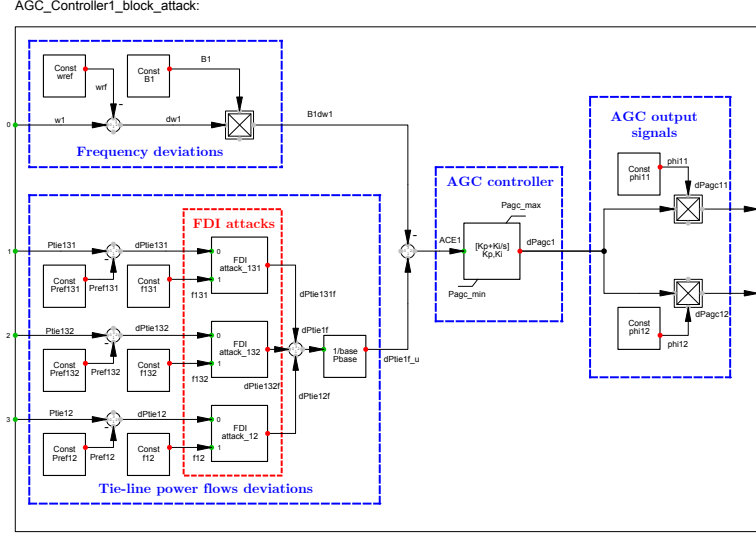


FIGURE 3. The block definition of AGC in PowerFactory.

as the excitation system in the type of IEEE Type 1, turbine-governor model (GOV) in the type of IEEE Type G1 (steam turbine) or IEEE Type G3 (hydro turbine). All the participated generators are with these controls in the test case.

The AGC controllers have been developed by the *DIgSILENT Simulation Language (DSL)*. The *composite frame* builds the connections between the inputs and outputs of the AGC model elements. Then the AGC *block definitions* for all areas can be created. For instance, Figure 3 illustrates the block definition of AGC in Area 1, which has four sub-blocks,

- *frequency deviations* block where the frequency deviations in p.u. multiplied by β_1 are calculated;
- *tie-line power flows deviations* block which computes the tie-line power flow deviations (normalized in p.u.) on the side of Area 1 for the power part of ACE_1 ;
- *AGC controller* block which performs the control action in (6) to generate ΔP_{agc_1} . To be noted, due to saturation, the limits of P_{agc}^{min} and P_{agc}^{max} are added for ΔP_{agc_1} ;
- *AGC output signals* block where the tuning signals for the participated generators in Area 1 for AGC are calculated based on each generator's participating factor.

The above block definitions are modeled using the *Standard Macros* of PowerFactory global *Library*. Moreover, in Figure 3, another block definition (in red diagram) corresponds to the FDI attack model for the study of this article,

- *FDI attacks* block where the FDI attack is implemented. Each block captures the feature of the stationary FDI attack¹ that it can add an “false” injection into the existing signal. One can specify the occurrence time and the attack values. This block definition is achieved by using the *digexfun* interface. With *digexfun*, we can define a specific DSL function (in C++) and create a dynamic link library *digexfun_*.dll* that the PF can load.

It has been noted in Figure 1 that there exist mismatches between the output y_p from the PF simulator and the one y from the DAE model. Indeed, the high-fidelity simulation model in the PF provides a more

¹The attack occurs as a constant bias injection ($f[k] = f$) on measurements at a specific time step ($k = k_{min}$), and it remains unchanged since then.

detailed description of the power system with AGCs, comparing with the “abstract” linear mathematical model (in the form of DAE) introduced in the preceding. In what follows we show how we can build a scalable data-assisted model-based diagnosis filter whose performance is robust to such output mismatches.

3. OPTIMIZATION-BASED CHARACTERIZATION OF THE DIAGNOSIS FILTER

3.1. Robust Anomaly Detection

We have restricted the diagnosis filter to a type of residual generator which has a linear transfer function in (3). Considering the DAE formulation in Section 2.1 for the model-based detection, the residual generator can be represented through the polynomial matrix equations. Thus for the transfer operator $R(q)$, we introduce $R(q) := a(q)^{-1}N(q)L(q)$. Then $N(q)$ with the dimension of n_r and a predefined order d_N becomes the filter design variable, if the scalar polynomial $a(q)$ with sufficient order to make $R(q)$ physically realizable is determined. We can further have

$$\begin{aligned} r[k] &= a(q)^{-1}N(q)L(q)y_p[k] \\ &= a(q)^{-1}N(q)L(q)(y[k] + e[k]) \\ &= -\underbrace{a(q)^{-1}N(q)H(q)x[k]}_{\text{(I)}} - \underbrace{a(q)^{-1}N(q)F(q)f[k]}_{\text{(II)}} \\ &\quad + \underbrace{a(q)^{-1}N(q)L(q)e[k]}_{\text{(III)}}, \end{aligned} \quad (7)$$

where term (II) is the desired contribution from the anomaly $f[\cdot]$. Ideally we would like to let the residual keep insensitive to term (I) and (III). For that purpose, first we need to “quantify” the effects of output mismatches on the filter residual. Thus for all $k \in \mathbb{N}$, let us define

$$r_e[k] := a(q)^{-1}N(q)L(q)e[k]. \quad (8)$$

Next, let us further denote the space of a discrete-time signal taking values in \mathbb{R}^n over the horizon of T (i.e., $k \in \{1, \dots, T\}$) by \mathcal{M}_T^n . We equip this space with an inner product and a corresponding norm as

$$\|v\|_{\mathcal{L}_2}^2 := \langle v, v \rangle, \quad \langle v, w \rangle := \sum_{k=1}^T v^\top[k]w[k], \quad (9)$$

where v, w are some elements in the space \mathcal{M}_T^n .

In view of (7) and (9), we introduce a scalable and robust diagnosis filter characterized by a class of residual generator which has the following features.

Definition 3.1 (Robust diagnosis filter). *Consider the residual generator represented via a polynomial vector $N(q)$ for a given $a(q)$. This residual generator is robust with respect to output mismatches and can detect all the plausible disruptive FDI attacks, if $N(q)$ is the optimal solution from*

$$\begin{aligned} \min_{N(q)} \quad & \|r_e\|_{\mathcal{L}_2}^2 \\ \text{s.t.} \quad & N(q)H(q) = 0, \\ & N(q)F(q)f \neq 0, \quad \forall f \in \mathcal{F}, \end{aligned} \quad (10)$$

where \mathcal{F} in term (II) is an admissible anomaly set. We emphasize that \mathcal{F} can be adjusted according to different anomaly scenarios where the convexity of the set is particularly desired from a computational perspective. For instance, in the scenario of disruptive univariate attack ($n_f = 1$), one can let \mathcal{F} be a set of $\{f \in \mathbb{R} : a_{\min} \leq$

$f \leq a_{max}$ where $a_{min}, a_{max} \in \mathbb{R}$ are non-zero variables decided by the attack targets on attack impact and undetectability. Similarly, for multivariate attacks ($n_f > 1$), we can introduce a set

$$\mathcal{F} = \{f \in \mathbb{R}^{n_f} : f = F_b^\top \alpha, \alpha \in \mathcal{A}\},$$

where $F_b := [f_1, f_2, \dots, f_d]$ represents a finite basis for the set of disruptive attacks and $\alpha := [\alpha_1, \alpha_2, \dots, \alpha_d]^\top \in \mathbb{R}^d$ contains the coefficients. $\mathcal{A} := \{\alpha \in \mathbb{R}^d \mid A\alpha \geq b\}$ with $A \in \mathbb{R}^{n_b \times d}$ and $b \in \mathbb{R}^{n_b}$ is a polytopic set to reflect attack targets on attack impact and undetectability.

3.2. Tractable optimization-based characterization under univariate attack

To explain the robustification scheme of the diagnosis filter, let us first consider the univariate attack scenario. Note that when there is no attack, the system outputs y_p and y only depend on the input of natural disturbances d . Thus for one instance of disturbances, d_i , one can have a specific signature e_i according to (4). For each $e_i \in \mathcal{M}_T^{n_y}$, a mismatch signature matrix $E_i \in \mathbb{R}^{n_y \times T}$ can be introduced,

$$E_i := [e_i[1], e_i[2], \dots, e_i[T]]. \quad (11)$$

Recall that the operator q acts as a time-shift operator: $qe_i[k] \rightarrow e_i[k+1]$. This operator is linear, and it can be translated as a matrix left-shift operator for matrix E_i : $qE_i = E_iD$ where D is a square matrix of order T . Following this and the definition of the residual r_e in (8), we have

$$a(q)r_e = N(q)L(q)E_i = \bar{N}\bar{L} \begin{bmatrix} I \\ qI \\ \vdots \\ q^{d_N}I \end{bmatrix} E_i = \bar{N}\bar{L}D_i, \quad (12)$$

where the matrices are defined as $\bar{N} := [N_0, N_1, \dots, N_{d_N}]$, $\bar{L} := \text{diag}[L, L, \dots, L]$ and $L(q) = L$. Here $D_i := [E_i^T, (E_iD)^T, \dots, (E_iD^{d_N})^T]^T$. Given a particular disturbance pattern d_i , the \mathcal{L}_2 -norm of the residual as defined in (9) can then be reformulated as a quadratic function,

$$\|r_{e_i}\|_{\mathcal{L}_2}^2 = \bar{N}Q_i\bar{N}^\top, \quad Q_i = (\bar{L}D_i)G(\bar{L}D_i)^\top, \quad (13)$$

where G is a positive semidefinite matrix with a dimension of T such that $G(p, u) = \langle a(q)^{-1}b_p, a(q)^{-1}b_u \rangle$ in which $b_p, b_u \in \mathcal{M}_T^1$ are the discrete time unit impulses.

Remark 3.2 (Training with multiple output mismatch signatures). *In order to robustify the diagnosis filter, it can be “trained” by utilizing the information of multiple instances of natural disturbances, i.e., $\{d_i\}_{i=1}^m$, in the normal system operations (without attacks). For each disturbance signature d_i , the output mismatch signature e_i and also the matrices E_i, D_i, Q_i can be computed from (11) to (13). Next, according to (10) in Definition 3.1 and also (13), the robust diagnosis filter has an optimization-based characterization where the objective function can be formulated to minimize $\bar{N}((1/m)\sum_{i=1}^m Q_i)\bar{N}^\top$ (average-cost viewpoint) or $\max_{i \leq m}(\bar{N}Q_i\bar{N}^\top)$ (worst-case viewpoint). We note that from computational perspective the average-cost is much more preferred.*

Theorem 3.3 (Tractable quadratic programming characterization). *Consider the polynomial matrices $H(q) = H_0 + H_1q$ and $F(q) = F$ where $H_0, H_1 \in \mathbb{R}^{n_r \times n_x}$ and $F \in \mathbb{R}^{n_r \times n_f}$ are constant matrices. The robust diagnosis filter introduced in (10) of Definition 3.1 for the univariate attack can be obtained by solving the program,*

$$\begin{aligned} \min_{\bar{N}} \quad & \bar{N} \left(\frac{1}{m} \sum_{i=1}^m Q_i \right) \bar{N}^\top \\ \text{s.t.} \quad & \bar{N}\bar{H} = 0, \\ & \|\bar{N}\bar{F}\|_\infty > 1, \end{aligned} \quad (14)$$

Algorithm 1 Diagnosis filter construction and validation for the simulator PF considering output mismatches.

- 1) **Pre-training:** For each $j \in \{1, \dots, 2d_N + 2\}$, solve the program (LP_{*j*}). Check if there exists $\gamma_j^* > 0$ and find the maximum of $\{\gamma_0^*, \gamma_1^*, \dots, \gamma_{2d_N+2}^*\}$.
 - 2) **Training phase:**
 - (i) For each instance d_i , run the PF simulations and compute the DAEs (in Matlab) to obtain y_p and y in the normal operations (without attacks). Calculate the matrices E_i , D_i , and Q_i according to (11) - (13).
 - (ii) For a number of m instances of disturbances, perform the same process in (i).
 - (iii) Set the initial value of γ_j in (14) to be $\max_{\{j \leq 2d_N+2\}} \gamma_j^*$ from **pre-training**. Solve (14) with the obtained matrix Q_i . Tune the value of γ_j until it reaches maximum.
 - 3) **Testing phase:** For another instance of disturbance with the same pattern as the ones in the **training phase**, run the PF simulation where the FDI attacks are also launched. Run the resulted diagnosis filter for detection.
-

where $\|\cdot\|_\infty$ denotes the infinite vector norm, and

$$\bar{H} := \begin{bmatrix} H_0 & H_1 & 0 & \cdots & 0 \\ 0 & H_0 & H_1 & 0 & \vdots \\ \vdots & 0 & \ddots & \ddots & 0 \\ 0 & \cdots & 0 & H_0 & H_1 \end{bmatrix}.$$

Similar to the matrix \bar{L} in (13), \bar{F} is defined as $\bar{F} := \text{diag}[F, F, \dots, F]$. Besides, a robust diagnosis filter from the program (14) but simply replacing the last non-convex constraint with the following one can have non-zero steady-state residual that approximates the attack value f ,

$$-a(1)^{-1} \sum_{i=0}^{d_N} N_i F = 1. \quad (15)$$

Proof. The key step is to observe that in (10) we can rewrite $N(q)H(q) = \bar{N}\bar{H}[I, qI, \dots, q^{d_N+1}I]^\top$, and $N(q)F(q) = \bar{N}\bar{F}[I, qI, \dots, q^{d_N}I]^\top$. Note that in the scenario of univariate attack, one can directly rewrite the last constraint of (10) as $N(q)F(q) \neq 0$, and scale this inequality to arrive at the one of (14). Next, if $\bar{N}\bar{H} = 0$, the diagnosis filter becomes $r[k] = -a(q)^{-1}N(q)F(q)f[k] + a(q)^{-1}N(q)L(q)e[k]$. If there is no output mismatch, the steady-state value of the filter residual under the univariate attack would be $-a(q)^{-1}N(q)F(q)f|_{q=1}$. Note that $N(1)F(1) = \sum_{i=0}^{d_N} N_i F$. Thus when there exist output mismatches, with the convex constraint of (15), the residual in its steady-state behavior could approximate f . \square

Strictly speaking, the optimization program (14) is not a quadratic program (QP) due to the last non-convex constraint. However, as explained by [12, Lemma 4.3], one can view (14) as a family of $d_N + 1$ standard QPs.

3.3. Extension to multivariate attack scenarios

Inspired by the techniques developed in [18], we further extend the preceding design of the robust diagnosis filter to the scenarios of multivariate attacks.

Corollary 3.4 (Robust diagnosis filter under multivariate attacks). *Consider the diagnosis filter in Definition 3.1 where the set of multivariate attacks is defined as $\mathcal{F} = \{f \in \mathbb{R}^{n_f} : f = F_b^\top \alpha, \alpha \in \mathcal{A}\}$ where*

$\mathcal{A} = \{\alpha \in \mathbb{R}^d \mid A\alpha \geq b\}$ (see Definition 3.1 for the denotation of these variables). Given $j \in \{1, \dots, 2d_N+2\}$, for each j , consider a family of the following quadratic programs,

$$\begin{aligned} \min_{\bar{N}, \lambda} \quad & \bar{N} \left(\frac{1}{m} \sum_{i=1}^m Q_i \right) \bar{N}^\top, \\ \text{s.t.} \quad & b^\top \lambda \geq \gamma_j, \\ & (-1)^j N_{\lfloor j/2 \rfloor} F F_b = \lambda^\top A, \\ & \bar{N} \bar{H} = 0, \lambda \geq 0, \end{aligned} \tag{QP}_j$$

where $\lfloor \cdot \rfloor$ is the ceiling function that maps the argument to the least integer. Then, the best solution of the programs (QP_j) among $j \in \{1, \dots, 2d_N+2\}$ solve the problem (10) in Definition 3.1 for the multivariate attack scenarios.

Proof. In the scenario of multivariate attacks, the two constraints in (10) can be characterized by the robust program,

$$\gamma^* := \max_{\bar{N} \in \mathcal{N}} \min_{\alpha \in \mathcal{A}} \{ \mathcal{J}(\bar{N}, \alpha) \}, \tag{16}$$

where the set $\mathcal{N} := \{ \bar{N} \in \mathbb{R}^{(d_N+1)n_r} \mid \bar{N} \bar{H} = 0 \}$. The source of the cost function $\mathcal{J}(\bar{N}, \alpha)$ is referred to [18, Section IV.B]. Then, according to [18, Theorem IV.3], we know that the robust program can be reformulated and relaxed to a set of linear programs (LPs),

$$\begin{aligned} \gamma_j^* := \max_{\bar{N}, \lambda} \quad & b^\top \lambda \\ \text{s.t.} \quad & (-1)^j N_{\lfloor j/2 \rfloor} F F_b = \lambda^\top A, \\ & \bar{N} \bar{H} = 0, \lambda \geq 0, \end{aligned} \tag{LP}_j$$

Namely, the solution to the program (LP_j) is a feasible solution to the robust program (16), and $\max_{\{j \leq 2d_N+2\}} \gamma_j^* \leq \gamma^*$. Then it is easy to obtain the finite (QP_j) for the multivariate attack scenarios. We conclude the proof by noting that if there exist a $\gamma_j^* > 0$, then a resulted filter from (LP_j) could detect all the admissible multivariate attacks in the set \mathcal{F} . \square

From Corollary 3.4, we can see that for any $j \in \{1, \dots, 2d_N+2\}$, if one can find a $\gamma_j > 0$ that (QP_j) is still feasible, then the solution to QP_j offers a robust diagnosis filter in the type of Definition 3.1 for multivariate attacks. For a better illustration, Algorithm 1 concludes the filter construction and validation process. In the “pre-training phase”, one needs to solve (LP_j) for each j to see if there exists $\gamma_j^* > 0$. If yes, next in the “training phase”, E_i , D_i and Q_i can be obtained from the simulation data in the normal operations for each disturbance signature d_i . Then the program (QP_j) needs to be solved and the resulted robust diagnosis filter can be “tested” to validate its performance.

In the end, we would like to highlight that the robust diagnosis filter from (QP_j) does not necessarily enforce a non-zero steady-state residual in multivariate attack scenarios. Regarding its steady-state behavior, the program (16) can be modified into $\mu^* := \max_{\{\bar{N} \in \mathcal{N}\}} \min_{\{\alpha \in \mathcal{A}\}} |\bar{N} \bar{F} \alpha|$ which has an exact convex reformulation. Then a similar treatment as the one mentioned in Corollary 3.4 can be deployed.

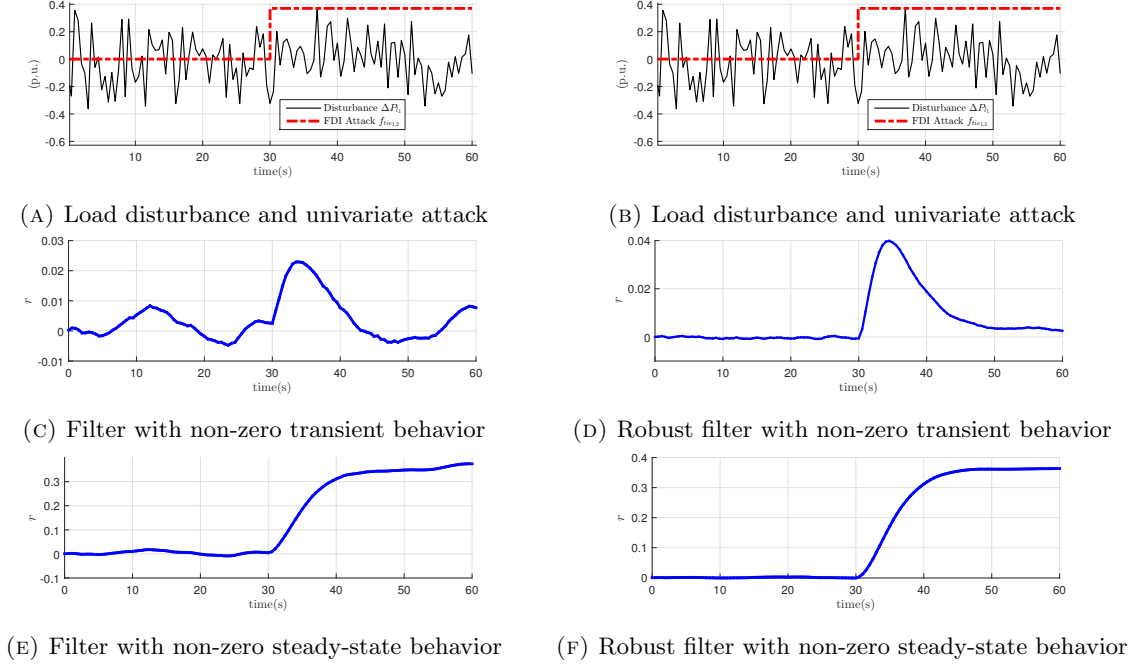


FIGURE 4. Residual signals of filters with or without robustification to output mismatches under a univariate attack.

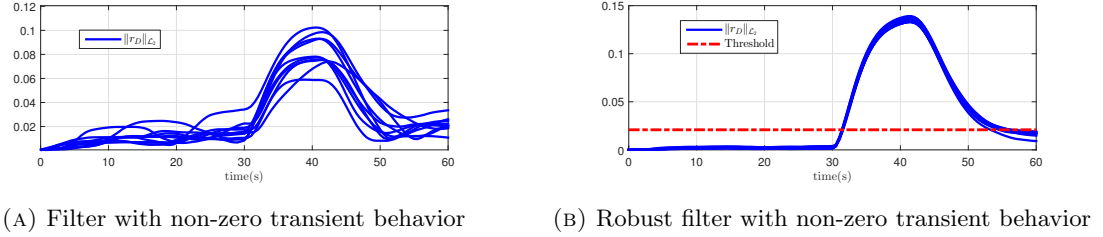


FIGURE 5. The “energy” of the residual signals for the filters with or without robustification under a univariate attack.

4. NUMERICAL RESULTS

4.1. Test System and Robust Detector Description

To validate the effectiveness of the proposed approach, the data-assisted model-based diagnosis filter has been implemented in the high-fidelity PF simulator to detect FDI attacks on the AGC measurements in the three-area 39-bus system. The AGC parameters of the linearized DAE model are referred to [4], and the specifications of the system model in PF are available at [20]. Following Algorithm 1, to obtain output mismatch signatures, we run the simulations to get the outputs y_p and y with the same input $d := \Delta P_l$ in the normal operations, where ΔP_l denotes the disturbance of load deviations. The adjustable degree of the residual generator is set to $d_N = 3$ which is much less than the order of the system dynamics; the scalar polynomial $a(q)$ is set to $a(q) = (q - p)^{d_N} / (1 - p)^{d_N}$ where p is a user-defined variable, acting as the pole of $R(q)$. We use CPLEX to solve all the corresponding optimization programs of this article.

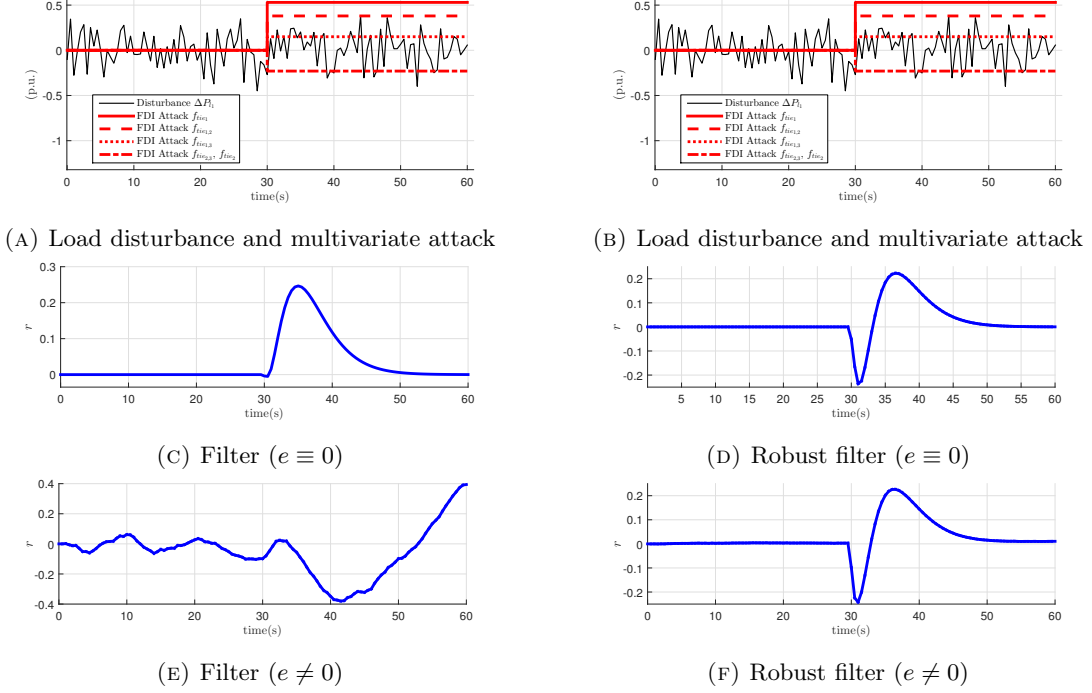


FIGURE 6. Residual signals of filters with or without robustification to output mismatches under multivariate attacks.

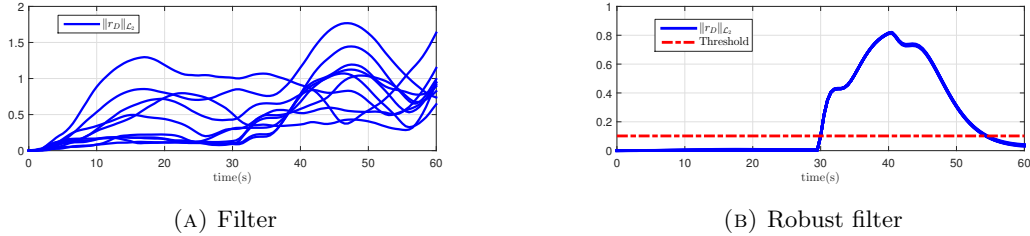


FIGURE 7. The “energy” of the residual signals for the filters with or without robustification.

4.2. Simulation Results

The first simulation considers the univariate attack scenario where an attacker has manipulated one tie-line power flow measurement $\Delta P_{tie_{1,2}}$ from $t = 30$ s in the horizon of 60 s. To challenge the filter, the disturbances are modeled as stochastic load patterns (load deviation of Load 4 in Area 1 is a random zero-mean Gaussian signal). A number of $m = 100$ load disturbance instances are generated for the “training phase” where for each load disturbance without attacks, the simulations with simulation time $t_s = 10$ s are conducted individually to obtain output mismatch signatures. The design variables \bar{N} are derived from (14) and to compare, a diagnosis filter without robustification is also computed with the objective function $\max_{\{\bar{N} \in \mathcal{N}\}} \|\bar{N}\bar{F}\|_\infty$ which can be transformed into finite LPs. In the “test phase”, the load disturbance has the same stochastic pattern with the ones in the “training phase”. The simulation results are referred Figure 4 and Figure 5. Indeed, the robust filter has significant improvements in mitigating the effects from output mismatches, while the filter without robustification fails. The robust filter can also have non-zero steady-state residual to approximate the univariate attack value. Figure 5 provides the residual results under 10 different realizations of load disturbances in the “testing phase”. It depicts the “energy” of the residual signals for the last 10s, namely

$\|r\|_{\mathcal{L}_2}[\cdot]$. Note that in Figure 5b the threshold is set to $\tau^* + 0.025$, where the square of τ^* equals to the maximum value of $\bar{N}Q_i\bar{N}$ in the 100 training instances ($i \in \{1, \dots, 100\}$; see (13)), and the added value is to avoid possible false alarms according to [13].

In the second simulation, we move to the scenario of multivariate attacks. There are 5 vulnerable measurements on the tie-lines between each areas, i.e., $\Delta P_{tie_{1,2}}$, $\Delta P_{tie_{1,3}}$, $\Delta P_{tie_{1,4}}$, $\Delta P_{tie_{2,3}}$ and $\Delta P_{tie_{2,4}}$, and correspondingly there exist 3 basis vectors in the spanning set \mathcal{F} : $f_1 = [0.1 \ 0 \ 0.1 \ 0 \ 0]^T$, $f_2 = [0.1 \ 0.15 \ 0.25 \ 0 \ 0]^T$, $f_3 = [0 \ 0 \ 0 \ 0.1 \ 0.1]^T$ (all in p.u.). Besides, for the set of disruptive multivariate attacks, the parameters are set to $A = \mathbf{1}^T$ and $b = 1.5$ in \mathcal{A} . Following Algorithm 1, the program (LP_j) is solved. The optimal value achieves maximum for $j = 2$ that $\gamma_2^* = 300$, which implies a robust diagnosis filter. Next, in the “training phase”, a number of 100 load disturbance instances are randomly generated. The program (QP_j) is solved for the robust diagnosis filter. For the derived \bar{N} , the multivariate attack coordinate vector α is obtained by solving the inner minimization of the program (16). In the “test phase”, simulations in PF are conducted that several realizations of load disturbances have been implemented and the multivariate attacks with α have been launched. The performance of the two filters (the filter from (QP_j) and the filter without robustification from (LP_j)) is validated with two sets of outputs: one from the DAE simulations ($e \equiv 0$) and another one from the PF simulations ($e \neq 0$). Figure 6 shows the simulation results of both diagnosis filters. We can see that both filters succeed for the case $e \equiv 0$. However, from Figure 6e and 6f, when there exist output mismatches, the robust filter still works effectively, while the filter without robustification totally fails by triggering “false alarms”. Besides, Figure 7 depicts the “energy” of the residual signals for the last 10s under 10 load disturbance instances. In Figure 7b, the threshold is set to $\tau^* + 0.1$ where the square of τ^* equals to the maximum value of $\bar{N}Q_i\bar{N}$ in the 100 training instances ($i \in \{1, \dots, 100\}$), and similarly the added value is to avoid possible false alarms. Note that when looking into the steady-state behavior of the filter, it turns out that $\mu^* = 0$, which indicates that the optimal multivariate attack in this case is a stealthy attack in the long-term horizon, with or without considering the output mismatch effects. However, one can still detect such attacks with a non-zero transient residual, as shown in Figure 6. In conclusion, these simulation results validate the effectiveness of our proposed solution.

5. CONCLUSION

In this article, we have proposed a feasible solution to the problem that arises from applying scalable model-based anomaly detectors in practice: there always exist mismatches between the output from the mathematical model and the one from the simulator (or the real electric power system). In the final reformulation, the DAE model-based information introduces feasible sets, and the simulation data forms the objective function to minimize the output mismatch effects, which could bridge the model-based and data-driven approaches.

REFERENCES

- [1] S. AHMED, Y. LEE, S.-H. HYUN, AND I. KOO, *Mitigating the impacts of covert cyber attacks in smart grids via reconstruction of measurement data utilizing deep denoising autoencoders*, *Energies*, 12 (2019).
- [2] A. AMELI, A. HOOSHYAR, E. F. EL-SAADANY, AND A. M. YOUSSEF, *Attack detection and identification for automatic generation control systems*, *IEEE Transactions on Power Systems*, 33 (2018), pp. 4760–4774.
- [3] A. AYAD, H. E. Z. FARAG, A. YOUSSEF, AND E. F. EL-SAADANY, *Detection of false data injection attacks in smart grids using recurrent neural networks*, in *IEEE PES ISGT Conference*, 2018, pp. 1–5.
- [4] H. BEVRANI, *Robust Power System Frequency Control*, *Power Electronics and Power Systems*, Springer, 2008.
- [5] S. X. DING, *Model-based fault diagnosis techniques: design schemes, algorithms, and tools*, Springer Science & Business Media, 2008.
- [6] J. HAO, R. J. PIECHOCKI, D. KALESHI, W. H. CHIN, AND Z. FAN, *Sparse malicious false data injection attacks and defense mechanisms in smart grids*, *IEEE Transactions on Industrial Informatics*, 11 (2015).

- [7] T. HUANG, B. SATCHIDANANDAN, P. R. KUMAR, AND L. XIE, *An online detection framework for cyber attacks on automatic generation control*, IEEE Transactions on Power Systems, 33 (2018), pp. 6816–6827.
- [8] H. JIANG, M. XIE, AND L. TANG, *Markov chain monte carlo methods for parameter estimation of the modified weibull distribution*, Journal of Applied Statistics, 35 (2008), pp. 647–658.
- [9] M. KHALAF, A. YOUSSEF, AND E. EL-SAADANY, *Joint detection and mitigation of false data injection attacks in AGC systems*, IEEE Transactions on Smart Grid, 10 (2019), pp. 4985–4995.
- [10] V. B. KRISHNA, G. A. WEAVER, AND W. H. SANDERS, *PCA-based method for detecting integrity attacks on advanced metering infrastructure*, in Quantitative Evaluation of Systems, Springer International Publishing, 2015.
- [11] M. N. KURT, O. OGUNDIJO, C. LI, AND X. WANG, *Online cyber-attack detection in smart grid: A reinforcement learning approach*, IEEE Transactions on Smart Grid, 10 (2019), pp. 5174–5185.
- [12] P. MOHAJERIN ESFAHANI AND J. LYGEROS, *A tractable fault detection and isolation approach for nonlinear systems with probabilistic performance*, IEEE Transactions on Automatic Control, 61 (2016), pp. 633–647.
- [13] P. MOHAJERIN ESFAHANI, T. SUTTER, AND J. LYGEROS, *Performance bounds for the scenario approach and an extension to a class of non-convex programs*, IEEE Transactions on Automatic Control, 60 (2015).
- [14] P. MOHAJERIN ESFAHANI, M. VRAKOPOULOU, G. ANDERSSON, AND J. LYGEROS, *A tractable nonlinear fault detection and isolation technique with application to the cyber-physical security of power systems*, in IEEE CDC, 2012.
- [15] M. NYBERG AND E. FRISK, *Residual generation for fault diagnosis of systems described by linear differential-algebraic equations*, IEEE Transactions on Automatic Control, 51 (2006), pp. 1995–2000.
- [16] H. M. ODENDAAL AND T. JONES, *Actuator fault detection and isolation: An optimised parity space approach*, Control Engineering Practice, 26 (2014), pp. 222–232.
- [17] M. OZAY, I. ESNAOLA, F. T. YARMAN VURAL, S. R. KULKARNI, AND H. V. POOR, *Machine learning methods for attack detection in the smart grid*, IEEE Transactions on Neural Networks and Learning Systems, 27 (2016).
- [18] K. PAN, P. PALENSKY, AND P. MOHAJERIN ESFAHANI, *From static to dynamic anomaly detection with application to power system cyber security*, IEEE Transactions on Power Systems, 35 (2020), pp. 1584–1596.
- [19] K. PAN, A. TEIXEIRA, C. D. LÓPEZ, AND P. PALENSKY, *Co-simulation for cyber security analysis: Data attacks against energy management system*, in IEEE SmartGridComm, 2017, pp. 253–258.
- [20] D. POWERFACTORY, *39 bus new england system*, tech. rep., DIgSILENT GmbH, 2018.
- [21] S. SRIDHAR AND M. GOVINDARASU, *Model-based attack detection and mitigation for automatic generation control*, IEEE Transactions on Smart Grid, (2014), pp. 580–591.
- [22] K. TIDRIRI, N. CHATTI, S. VERRON, AND T. TIPLICA, *Bridging data-driven and model-based approaches for process fault diagnosis and health monitoring: A review of researches and future challenges*, Annual Reviews in Control, 42 (2016).
- [23] Y. WADHAWAN, A. ALMAJALI, AND C. NEUMAN, *A comprehensive analysis of smart grid systems against cyber-physical attacks*, Electronics, (2018).
- [24] T. WEI, X. CHEN, X. LI, AND Q. ZHU, *Model-based and data-driven approaches for building automation and control*, in IEEE/ACM ICCAD, 2018, pp. 1–8.
- [25] J. YU, Y. HOU, AND V. LI, *Online false data injection attack detection with wavelet transform and deep neural networks*, IEEE Transactions on Industrial Informatics, (2018).